jugate-base mechanism, ICB,[37] is operative, in the latter the ligand, blocked by a proton, is responsible for the retardation. This behavior seems to be always operative when an internal hydrogen bond at the reaction site is present, for which we propose the designation "internal hydrogen bond mechanism".

Acknowledgment. The present work has been performed with the financial support of the CNR (Rome). The authors wish to thank Professor B. Perlmutter-Hayman for stimulating and helpful discussions.

Registry No. H_2ClSAL, 321-14-2; H_2SSAL, 97-05-2; H_2NSAL, 96-97-9; H_2SAL, 69-72-7; Ni^{2+}, 14701-22-5; Co^{2+}, 22541-53-3.

(37) Rorabacher, D. B. *Inorg. Chem.* **1966**, *5*, 1891. Taylor, R. W.; Stepien, H. K.; Rorabacher, D. B. *Ibid.* **1974**, *13*, 1282.

Contribution from the Institute of Materials Science and Department of Chemistry, University of Connecticut, Storrs, Connecticut 06268

Crystal Structure of Ferric Molybdate, $Fe_2(MoO_4)_3$

M. H. RAPPOSCH, J. B. ANDERSON, and E. KOSTINER*

Received February 8, 1980

Single crystals of $Fe_2(MoO_4)_3$ have been grown by hydrothermal techniques from 0.75 M HCl solution and by flux techniques from K_2MoO_4–MoO_3–B_2O_3. $Fe_2(MoO_4)_3$ crystallizes in the space group $P2_1$ with a = 15.693 (3) Å, b = 9.235 (1) Å, c = 18.218 (4) Å, and β = 125.21 (1)°. Full three-dimensional least-squares isotropic refinement using counter diffractometer data converged to R = 0.041 (R_w = 0.055) for 2464 observed independent data. The relationship of this structure to that of $Sc_2(WO_4)_3$ is discussed. Magnetic susceptibility measurements are indicative of an antiferromagnetic material with an ordering temperature below 80 K (Θ = −62.7 K).

Introduction

Molybdates and tungstates of trivalent metal ions, $M_2(XO_4)_3$, have been classified[1] according to the coordination polyhedra about the metal atoms. In particular, molybdates of the smaller lanthanides as well as those of Al, Cr, Fe, Sc, and In are reported[1] to form with the C-type structure, characterized by tetrahedral MoO_4 groups and six-coordinated trivalent metal ions. The prototype of this structure is the orthorhombic tungstate $Sc_2(WO_4)_3$, described by Abrahams and Bernstein.[2]

Of the molybdates, structure determinations have been reported for $In_2(MoO_4)_3$[3] and $Fe_2(MoO_4)_3$,[4] which are described as crystallizing in the space group $P2_1/a$. Monoclinic $Fe_2(MoO_4)_3$ has also been reported[5] to reversibly transform to an orthorhombic form at 518 °C.

We have grown single crystals of ferric molybdate of suitable size and quality for X-ray diffraction studies by both high-temperature flux and hydrothermal techniques and present the results of our structure refinement of this compound. A preliminary report of this work has been presented.[6]

Experimental Section

Synthesis and Crystal Growth. Nutrient material was prepared by mixing stoichiometric aqueous solutions of reagent grade ferric nitrate and ammonium molybdate, boiling the mixture gently for 30 min, and then filtering the precipitate. The solid product was dried at 110 °C, ground thoroughly, and sintered overnight at 800 °C. The resulting yellow-green powder gave an X-ray powder diffraction pattern identical with that reported in the literature.[5] This nutrient proved to be far superior to stoichiometric mixtures of Fe_2O_3 and MoO_3 since it eliminated any free Fe_2O_3 upon which $Fe_2(MoO_4)_3$ is prone to nucleate.

After preliminary experiments using the high-temperature flux technique, a flux consisting of 13.35 mol % K_2MoO_4, 13.35 mol % MoO_3, and 73.30 mol % B_2O_3 was selected. Optimum conditions for the growth of $Fe_2(MoO_4)_3$ by this technique require that a 4–6 mol % solution of the nutrient in this flux be soaked for 12–24 h at 800 °C and then cooled at 15 °C/h to ambient temperature. The resulting crystals, separated from the flux by boiling water, were yellow-green and, for the most part, exhibited a largely bladelike habit. Occasionally, some of these crystals formed as well-defined rectangular tablets with beveled edges.

Initial attempts to grow single crystals of $Fe_2(MoO_4)_3$ by the hydrothermal technique were based on a method developed by Klevtsov.[7] Charges of 50 mg of a stoichiometric mixture of the component oxides (1:3 Fe_2O_3:MoO_3) along with a mineralizer charge of 0.02–0.20 mL of a 6 wt % $FeCl_3$ solution were sealed in 5-mm-diameter gold tubes 5 cm long and contained in cold-seal autoclaves (TemPress MRA 114R) operating at 3–60 kpsi and 450–480 °C. It was found that, under these conditions, successful growth runs could last only 2 days due to the deterioration of the gold capsules in the highly acidic halide mineralizer. For optimal growth period and for elimination of nucleation and contamination problems the precipitated nutrient material was substituted for the oxide mixture and the mineralizer (which hydrolyzes to form Fe_2O_3) was changed to a 0.25–0.75 M HCl solution. At pressures below ~28 kpsi, transparent, strongly pleochroic, lemon yellow-green crystals form up to 0.30 mm in maximum dimension. These crystals often exhibit the characteristic rectangular tablet habit of flux-grown crystals. At pressures above this range, large (1–2 mm) green crystals form. Precession photographs indicate, however, that these "crystals" are often twinned and are in most instances nearly polycrystalline.

Magnetic Susceptibility. Magnetic data were recorded in the temperature range 84–303 K with a Faraday balance of the type described by Morris and Wold.[8] Absence of ferromagnetic impurities

* To whom correspondence should be addressed at the Department of Chemistry.

(1) K. Nassau, H. J. Levinstein, and G. M. Loiacono, *J. Phys. Chem. Solids*, **26**, 1805 (1965).
(2) S. C. Abrahams and J. L. Bernstein, *J. Chem. Phys.*, **45**, 2745 (1966).
(3) L. M. Plyasova, R. F. Klevtsova, S. V. Borisov, and L. M. Kefeli, *Sov. Phys.—Crystallogr.* (*Engl. Transl.*), **13**, 29 (1968).
(4) L. M. Plyasova, R. F. Klevtsova, S. V. Borisov, and L. M. Kefeli, *Sov. Phys.—Dokl.* (*Engl. Transl.*), **11**, 189 (1966).
(5) L. M. Plyasova, *J. Struct. Chem.* (*Engl. Transl.*), **17**, 637 (1976).
(6) M. H. Rapposch, E. Kostiner, and J. B. Anderson, Abstracts, 178th National Meeting of the American Chemical Society, Washington, DC, Sept 1979, No. INOR 195.
(7) P. V. Klevtsov, *Sov. Phys.—Crystallogr.* (*Engl. Transl.*), **10**, 370 (1965).
(8) B. L. Morris and A. Wold, *Rev. Sci. Instrum.*, **89**, 1937 (1968).

0020-1669/80/1319-3531$01.00/0

Table I. Fractional Atomic Coordinates and Isotropic Thermal Parameters[a]

atom	*x*	*y*	*z*	*B*, Å^2	atom	*x*	*y*	*z*	*B*, Å^2
Fe(1)	0.1302 (6)	0.9655	0.3187 (5)	0.49 (13)	O(8)	0.077 (3)	0.302 (4)	0.091 (2)	1.28 (74)
Fe(1′)	0.6317 (7)	−0.4657 (4)	0.3193 (6)	0.87 (14)	O(8′)	0.579 (3)	0.192 (4)	0.097 (2)	0.86 (68)
Fe(2)	0.1225 (6)	0.4610 (12)	0.0473 (5)	0.83 (14)	O(9)	0.161 (2)	0.611 (3)	−0.001 (1)	−0.21 (44)
Fe(2′)	0.6182 (6)	0.0417 (11)	0.0435 (5)	0.36 (13)	O(9′)	0.675 (3)	−0.115 (4)	0.002 (2)	2.70 (79)
Fe(3)	−0.1305 (6)	0.4742 (11)	0.1858 (5)	0.45 (14)	O(10)	0.136 (2)	0.313 (3)	0.974 (2)	−0.10 (50)
Fe(3′)	0.3691 (7)	0.0261 (12)	0.1845 (6)	0.90 (15)	O(10′)	0.645 (3)	0.195 (5)	0.980 (3)	3.20 (93)
Fe(4)	−0.1430 (6)	0.9790 (12)	0.4175 (5)	0.45 (13)	O(11)	0.244 (2)	0.099 (3)	0.170 (2)	0.91 (58)
Fe(4′)	0.3554 (6)	−0.4874 (12)	0.4151 (5)	0.90 (14)	O(11′)	0.732 (2)	0.415 (3)	0.171 (2)	1.14 (62)
Mo(1)	0.7395 (3)	0.2476 (10)	0.4848 (3)	0.63 (8)	O(12)	0.027 (2)	0.005 (3)	0.061 (2)	0.92 (57)
Mo(1′)	0.2470 (3)	0.2549 (10)	0.4897 (3)	0.62 (8)	O(12′)	0.525 (2)	0.499 (3)	0.047 (2)	1.41 (64)
Mo(2)	0.1112 (3)	0.1300 (10)	0.1398 (3)	0.72 (9)	O(13)	0.157 (2)	0.810 (3)	0.405 (2)	−0.21 (49)
Mo(2′)	0.6105 (3)	0.3746 (10)	0.1345 (3)	0.40 (8)	O(13′)	0.650 (3)	−0.315 (4)	0.409 (2)	2.25 (77)
Mo(3)	−0.1110 (3)	0.1112 (10)	0.2492 (3)	0.50 (8)	O(14)	0.173 (2)	0.110 (3)	0.418 (2)	0.28 (51)
Mo(3′)	0.3901 (4)	0.3870 (10)	0.2499 (3)	0.77 (9)	O(14′)	0.666 (3)	0.385 (4)	0.409 (2)	2.14 (72)
Mo(4)	−0.2494 (3)	0.7433 (10)	0.0194 (3)	0.71 (8)	O(15)	0.091 (3)	0.825 (5)	0.227 (3)	3.18 (94)
Mo(4′)	0.2541 (3)	−0.2462 (10)	0.0198 (3)	0.43 (8)	O(15′)	0.596 (2)	−0.310 (3)	0.227 (2)	−0.27 (49)
Mo(5)	−0.0995 (3)	0.6193 (10)	0.3835 (3)	0.44 (8)	O(16)	0.108 (3)	0.127 (4)	0.236 (2)	2.52 (83)
Mo(5′)	0.4009 (3)	−0.1118 (10)	0.3868 (3)	0.85 (9)	O(16′)	0.608 (2)	0.388 (3)	0.230 (2)	0.04 (52)
Mo(6)	0.1012 (3)	0.6314 (10)	0.2136 (3)	0.50 (8)	O(17)	−0.015 (2)	− 0.017 (3)	0.282 (2)	0.79 (50)
Mo(6′)	0.6017 (3)	−0.1291 (10)	0.2118 (3)	0.60 (8)	O(17′)	0.481 (2)	0.525 (3)	0.264 (2)	1.14 (55)
O(1)	−0.176 (2)	0.382 (4)	0.071 (2)	1.52 (67)	O(18)	0.221 (2)	0.574 (3)	0.315 (2)	1.62 (64)
O(1′)	0.310 (2)	0.120 (3)	0.067 (2)	0.63 (55)	O(18′)	0.703 (2)	−0.056 (3)	0.310 (2)	0.91 (54)
O(2)	−0.213 (2)	0.658 (4)	0.115 (2)	2.00 (71)	O(19)	−0.137 (3)	0.104 (5)	0.332 (2)	1.99 (78)
O(2′)	0.302 (2)	−0.156 (3)	0.126 (2)	0.11 (48)	O(19′)	0.370 (2)	0.390 (4)	0.336 (2)	1.01 (66)
O(3)	−0.067 (2)	0.280 (3)	0.240 (2)	0.50 (53)	O(20)	−0.092 (2)	0.804 (3)	0.400 (2)	1.08 (56)
O(3′)	0.435 (2)	0.206 (3)	0.251 (2)	0.79 (57)	O(20′)	0.407 (2)	−0.304 (3)	0.384 (2)	1.63 (63)
O(4)	−0.093 (2)	0.574 (3)	0.295 (2)	0.55 (54)	O(21)	−0.211 (3)	0.140 (4)	0.443 (3)	4.00 (91)
O(4′)	0.422 (2)	−0.053 (3)	0.306 (2)	1.17 (62)	O(21′)	0.304 (2)	0.350 (3)	0.445 (2)	0.26 (45)
O(5)	−0.003 (2)	0.541 (3)	0.201 (2)	1.35 (62)	O(22)	−0.157 (2)	0.857 (3)	0.501 (1)	0.17 (45)
O(5′)	0.487 (2)	−0.040 (3)	0.186 (2)	1.21 (59)	O(22′)	0.328 (3)	−0.370 (4)	0.495 (2)	3.01 (80)
O(6)	−0.226 (2)	0.076 (3)	0.137 (2)	0.65 (52)	O(23)	−0.220 (3)	0.561 (4)	0.359 (2)	1.60 (75)
O(6′)	0.273 (2)	0.428 (3)	0.151 (2)	0.97 (56)	O(23′)	0.284 (3)	−0.049 (4)	0.366 (2)	1.80 (73)
O(7)	0.105 (2)	0.605 (4)	0.119 (2)	1.97 (74)	O(24)	0.002 (2)	0.542 (3)	0.492 (2)	0.19 (47)
O(7′)	0.620 (2)	−0.096 (3)	0.125 (2)	0.54 (57)	O(24′)	0.498 (3)	−0.035 (4)	0.478 (2)	3.52 (93)

[a] Numbers in parentheses are estimated standard deviations in the last significant figure.

was verified by the Honda–Owens method.[9] Diamagnetic corrections[10] were applied to the raw data.

X-ray Diffraction Data. X-ray powder diffraction patterns taken of crystals produced by both of the above techniques indicate that they are identical. A flux-grown single crystal exhibiting rectangular habit with dimensions 0.1 × 0.2 × 0.16 mm was selected for space group determination. During the course of obtaining a complete set of precession photographs of this crystal, three interesting features were noted, the first two of which were already reported by Plyasova et al.[4] When examined in the morphological setting, the crystal exhibited a distinct pseudoorthorhombic subcell (space group *Pnca*) with dimensions $a = 9.20$, $b = 12.78$, and $c = 9.08$ Å. Second, when long-exposure cone-axis photographs along this c axis were taken, very weak odd levels were observed, indicating a doubling of the axis. The third and most crucial feature was observed only after careful inspection of a 72-h zero-level photograph of the monoclinic a–c net. Careful determination of systematic absences revealed the true symmetry to be $P2_1$ rather than the previously reported $P2_1/a$.

A hydrothermally grown crystal, prepared from 50 mg of a mixture of the component oxides in 0.1 mL of 0.75 M HCl solution at 23.7 kpsi and 450 °C, ground to a sphere with radius $r = 0.0078$ (8) cm, was used for data collection.

Lattice parameters were determined in a PICK-II least-squares refinement program, by using 24 reflections within the angular range $35° < 2\theta < 43°$; the reflections were automatically centered on a Picker FACS-I four-circle diffractometer using Mo Kα_1 radiation (λ = 0.709 30 Å). At 25 °C the lattice parameters for the unit cell were found to be $a = 15.693$ (3) Å, $b = 9.235$ (1) Å, $c = 18.218$ (4) Å, and $\beta = 125.21$ (1)°, where the figures in parentheses represent the standard deviations in the last reported figure. The calculated volume is 2157.2 Å^3, giving a calculated density, with $Z = 8$, of 3.642 g cm^{-3}.

Diffraction intensities were measured by using Zr-filtered Mo Kα radiation at a takeoff angle of 1.5° with the diffractometer operating in the ω-scan mode. Ten-second background counts were taken at both ends of a 1.4° θ–2θ offset corrected for dispersion. Of the 3083 independent data investigated in the angular range $2\theta < 45°$, 2464 were considered observable according to the criterion $|F_o| > 3.0\sigma_F$, where σ_F is defined as $0.02|F_o| + [C + k^2B]^{1/2}/2|F_o|Lp$; the total scan count is C, k is the ratio of scanning time to the total background time, and B is the total background count. Three standard reflections were systematically monitored; the maximum variation in intensity observed was never greater than ±3% over the data collection period.

The intensity data were corrected for Lorentz and polarization effects, secondary extinction, and anomalous dispersion. The absorption correction[11] was made for a spherical crystal with $\mu r = 0.47$. The maximum relative absorption correction applied was 0.65% of $|F_o|$.

Refinement of the Structure. Using the space group $P2_1/a$ and the positional parameters reported by Plyasova et al.[4] as a trial structure, a full-matrix least-squares refinement[12] with a $1/\sigma^2$ weighting scheme and zerovalent scattering factors[13] for Fe, Mo, and O was carried out. In the initial stages of refinement, the positional parameters and isotropic temperature factors of the ten unique metal atoms in this space group were refined in the absence of oxygens to $R = 0.19$. Introduction of 24 oxygen atoms and subsequent isotropic refinement further reduced R to 0.055. Since the least-squares program could not deal with more than 198 variables simultaneously, this and subsequent refinement cycles were carried out by alternating the metal and then the oxygen parameters.

With use of these data, a Fourier difference map was computed which revealed a single peak with an intensity comparable to that of an oxygen peak. This fact suggested that an oxygen was misplaced,

(9) K. Honda, *Ann. Phys. (Leipzig)*, **32**, 1048 (1912); M. Owens, *ibid.*, **37**, 657 (1912).
(10) P. W. Selwood, "Magnetochemistry", 2nd ed., Interscience, New York, 1956, p 78.
(11) "International Table for X-Ray Crystallography", Vol. II, Kynoch Press, Birmingham, England, 1968, p 295.
(12) W. R. Busing, K. O. Martin, and H. A. Levy, "ORFLS", Report ORNL-TM-305, Oak Ridge National Laboratory, Oak Ridge, TN, 1962.
(13) "International Tables for X-Ray Crystallography", Vol. IV, Kynoch Press, Birmingham, England, 1974, p 99.

Table II. Bond Distances (A), Bond Angles (Deg), and Polyhedral Edge Lengths (A) for Molybdenum Tetrahedra[a]

	dist	angle	edge
Mo(1) Tetrahedron			
Mo(1)-O(21)	1.70 (4)		
Mo(1)-O(22′)	1.70 (4)		
Mo(1)-O(14′)	1.74 (4)		
Mo(1)-O(13)	1.80 (3)		
O(21)-Mo(1)-O(22′)		103 (2)	2.67 (5)
O(21)-Mo(1)-O(14′)		110 (2)	2.81 (5)
O(21)-Mo(1)-O(13)		110 (1)	2.86 (5)
O(22′)-Mo(1)-O(14′)		115 (2)	2.90 (5)
O(22′)-Mo(1)-O(13)		104 (1)	2.75 (4)
O(14′)-Mo(1)-O(13)		114 (1)	2.97 (4)
Mo(1′) Tetrahedron			
Mo(1′)-O(13′)	1.73 (4)		
Mo(1′)-O(21′)	1.74 (2)		
Mo(1′)-O(14)	1.76 (3)		
Mo(1′)-O(22)	1.79 (2)		
O(13′)-Mo(1′)-O(21′)		106 (1)	2.77 (4)
O(13′)-Mo(1′)-O(14)		108 (2)	2.83 (4)
O(13′)-Mo(1′)-O(22)		113 (1)	2.95 (4)
O(21′)-Mo(1′)-O(14)		110 (1)	2.86 (4)
O(21′)-Mo(1′)-O(22)		115 (1)	2.98 (4)
O(14)-Mo(1′)-O(22)		105 (1)	2.81 (4)
Mo(2) Tetrahedron			
Mo(2)-O(12)	1.72 (3)		
Mo(2)-O(8)	1.75 (4)		
Mo(2)-O(16)	1.78 (4)		
Mo(2)-O(11)	1.85 (3)		
O(12)-Mo(2)-O(8)		109 (1)	2.82 (4)
O(12)-Mo(2)-O(16)		112 (2)	2.90 (4)
O(12)-Mo(2)-O(11)		109 (1)	2.91 (4)
O(8)-Mo(2)-O(16)		110 (2)	2.89 (5)
O(8)-Mo(2)-O(11)		105 (1)	2.85 (5)
O(16)-Mo(2)-O(11)		112 (1)	3.01 (4)
Mo(2′) Tetrahedron			
Mo(2′)-O(11′)	1.66 (3)		
Mo(2′)-O(16′)	1.77 (3)		
Mo(2′)-O(8′)	1.78 (3)		
Mo(2′)-O(12′)	1.79 (3)		
O(11′)-Mo(2′)-O(16′)		105 (1)	2.72 (4)
O(11′)-Mo(2′)-O(8′)		112 (1)	2.84 (4)
O(11′)-Mo(2′)-O(12′)		109 (1)	2.79 (4)
O(16′)-Mo(2′)-O(8′)		107 (1)	2.84 (4)
O(16′)-Mo(2′)-O(12′)		113 (1)	2.97 (4)
O(8′)-Mo(2′)-O(12′)		112 (1)	2.95 (4)
Mo(3) Tetrahedron			
Mo(3)-O(17)	1.73 (2)		
Mo(3)-O(3)	1.75 (3)		
Mo(3)-O(19)	1.77 (4)		
Mo(3)-O(6)	1.81 (2)		
O(17)-Mo(3)-O(3)		109 (1)	2.84 (4)
O(17)-Mo(3)-O(19)		105 (2)	2.78 (4)
O(17)-Mo(3)-O(6)		112 (1)	2.93 (3)
O(3)-Mo(3)-O(19)		114 (2)	2.96 (5)
O(3)-Mo(3)-O(6)		104 (1)	2.81 (3)
O(19)-Mo(3)-O(6)		113 (1)	2.98 (4)
Mo(3′) Tetrahedron			
Mo(3′)-O(6′)	1.72 (3)		
Mo(3′)-O(19′)	1.76 (3)		
Mo(3′)-O(3′)	1.81 (3)		
Mo(3′)-O(17′)	1.81 (3)		
O(6′)-Mo(3′)-O(19′)		107 (1)	2.79 (4)
O(6′)-Mo(3′)-O(3′)		113 (1)	2.94 (4)
O(6′)-Mo(3′)-O(17′)		106 (1)	2.82 (3)
O(19′)-Mo(3′)-O(3′)		106 (1)	2.84 (4)
O(19′)-Mo(3′)-O(17′)		113 (1)	2.97 (4)
O(3′)-Mo(3′)-O(17′)		113 (1)	3.01 (5)
Mo(4) Tetrahedron			
Mo(4)-O(9′)	1.68 (4)		
Mo(4)-O(2)	1.69 (3)		
Mo(4)-O(1′)	1.72 (3)		
Mo(4)-O(10)	1.82 (3)		
O(9′)-Mo(4)-O(2)		110 (2)	2.75 (5)
O(9′)-Mo(4)-O(1′)		113 (1)	2.84 (5)
O(9′)-Mo(4)-O(10)		107 (2)	2.82 (4)
O(2)-Mo(4)-O(1′)		108 (1)	2.76 (4)
O(2)-Mo(4)-O(10)		111 (1)	2.89 (4)
O(1′)-Mo(4)-O(10)		107 (1)	2.85 (4)
Mo(4′) Tetrahedron			
Mo(4′)-O(10′)	1.66 (4)		
Mo(4′)-O(1)	1.82 (3)		
Mo(4′)-O(2′)	1.83 (2)		
Mo(4′)-O(9)	1.83 (2)		
O(10′)-Mo(4′)-O(1)		111 (2)	2.87 (5)
O(10′)-Mo(4′)-O(2′)		109 (2)	2.84 (5)
O(10′)-Mo(4′)-O(9)		114 (2)	2.93 (5)
O(1)-Mo(4′)-O(2′)		109 (1)	2.96 (4)
O(1)-Mo(4′)-O(9)		104 (1)	2.87 (4)
O(2′)-Mo(4′)-O(9)		110 (1)	3.00 (4)
Mo(5) Tetrahedron			
Mo(5)-O(4)	1.72 (2)		
Mo(5)-O(20)	1.72 (2)		
Mo(5)-O(23)	1.76 (3)		
Mo(5)-O(24)	1.82 (2)		
O(4)-Mo(5)-O(20)		112 (1)	2.85 (4)
O(4)-Mo(5)-O(23)		108 (1)	2.82 (4)
O(4)-Mo(5)-O(24)		115 (1)	2.99 (4)
O(20)-Mo(5)-O(23)		108 (2)	2.83 (4)
O(20)-Mo(5)-O(24)		106 (1)	2.83 (4)
O(23)-Mo(5)-O(24)		107 (1)	2.88 (4)
Mo(5′) Tetrahedron			
Mo(5′)-O(24′)	1.63 (4)		
Mo(5′)-O(23′)	1.74 (3)		
Mo(5′)-O(4′)	1.78 (3)		
Mo(5′)-O(20′)	1.78 (3)		
O(24′)-Mo(5′)-O(23′)		109 (2)	2.74 (5)
O(24′)-Mo(5′)-O(4′)		102 (2)	2.64 (4)
O(24′)-Mo(5′)-O(20′)		115 (2)	2.89 (5)
O(23′)-Mo(5′)-O(4′)		113 (1)	2.94 (4)
O(23′)-Mo(5′)-O(20′)		113 (2)	2.94 (5)
O(4′)-Mo(5′)-O(20′)		104 (2)	2.80 (4)
Mo(6) Tetrahedron			
Mo(6)-O(5)	1.72 (3)		
Mo(6)-O(7)	1.78 (3)		
Mo(6)-O(18)	1.79 (3)		
Mo(6)-O(15)	1.82 (4)		
O(5)-Mo(6)-O(7)		111 (1)	2.89 (4)
O(5)-Mo(6)-O(18)		110 (1)	2.88 (4)
O(5)-Mo(6)-O(15)		110 (2)	2.91 (5)
O(7)-Mo(6)-O(18)		111 (1)	2.94 (4)
O(7)-Mo(6)-O(15)		108 (2)	2.92 (5)
O(18)-Mo(6)-O(15)		106 (2)	2.89 (5)
Mo(6′) Tetrahedron			
Mo(6′)-O(18′)	1.70 (2)		
Mo(6′)-O(15′)	1.71 (3)		
Mo(6′)-O(5′)	1.78 (3)		
Mo(6′)-O(7′)	1.79 (3)		
O(18′)-Mo(6′)-O(15′)		109 (1)	2.77 (4)
O(18′)-Mo(6′)-O(5′)		107 (1)	2.79 (4)
O(18′)-Mo(6′)-O(7′)		109 (1)	2.85 (4)
O(15′)-Mo(6′)-O(5′)		111 (1)	2.87 (4)
O(15′)-Mo(6′)-O(7′)		111 (1)	2.89 (4)
O(5′)-Mo(6′)-O(7′)		109 (1)	2.91 (4)

[a] Numbers in parentheses are estimated standard deviations in the last significant figure.

Table III. Bond Distances (Å), Bond Angles (Deg), and Polyhedral Edge Lengths (Å) for Iron Octahedra[a]

	dist	angle	edge
Fe(1) Polyhedron			
Fe(1)-O(15)	1.91 (4)		
Fe(1)-O(17)	1.98 (2)		
Fe(1)-O(13)	1.99 (3)		
Fe(1)-O(16)	2.00 (4)		
Fe(1)-O(14)	2.03 (3)		
Fe(1)-O(23′)	2.06 (3)		
O(15)-Fe(1)-O(17)		92 (1)	2.81 (5)
O(15)-Fe(1)-O(13)		91 (1)	2.79 (5)
O(15)-Fe(1)-O(16)		91 (2)	2.80 (6)
O(15)-Fe(1)-O(23′)		92 (2)	2.85 (5)
O(17)-Fe(1)-O(13)		90 (1)	2.81 (3)
O(17)-Fe(1)-O(16)		91 (1)	2.83 (4)
O(17)-Fe(1)-O(14)		88 (1)	2.79 (4)
O(13)-Fe(1)-O(14)		88 (1)	2.78 (4)
O(13)-Fe(1)-O(23′)		87 (1)	2.80 (4)
O(16)-Fe(1)-O(14)		90 (1)	2.86 (4)
O(16)-Fe(1)-O(23′)		91 (1)	2.90 (5)
O(14)-Fe(1)-O(23′)		88 (1)	2.83 (4)
Fe(1′) Polyhedron			
Fe(1′)-O(14′)	1.96 (4)		
Fe(1′)-O(17′)	1.97 (3)		
Fe(1′)-O(16′)	1.98 (3)		
Fe(1′)-O(23)	2.01 (3)		
Fe(1′)-O(15′)	2.03 (3)		
Fe(1′)-O(13′)	2.03 (4)		
O(14′)-Fe(1′)-O(17′)		94 (1)	2.87 (4)
O(14′)-Fe(1′)-O(16′)		92 (1)	2.84 (4)
O(14′)-Fe(1′)-O(23)		95 (1)	2.93 (5)
O(14′)-Fe(1′)-O(13′)		88 (1)	2.78 (5)
O(17′)-Fe(1′)-O(16′)		87 (1)	2.72 (4)
O(17′)-Fe(1′)-O(15′)		86 (1)	2.73 (4)
O(17′)-Fe(1′)-O(13′)		91 (1)	2.85 (4)
O(16′)-Fe(1′)-O(23)		90 (1)	2.84 (4)
O(16′)-Fe(1′)-O(15′)		88 (1)	2.79 (4)
O(23)-Fe(1′)-O(15′)		85 (1)	2.74 (4)
O(23)-Fe(1′)-O(13′)		92 (1)	2.91 (5)
O(15′)-Fe(1′)-O(13′)		92 (1)	2.91 (4)
Fe(2) Polyhedron			
Fe(2)-O(9)	1.93 (2)		
Fe(2)-O(8)	1.99 (4)		
Fe(2)-O(7)	1.99 (3)		
Fe(2)-O(10)	2.02 (3)		
Fe(2)-O(6′)	2.02 (3)		
Fe(2)-O(12)	2.05 (4)		
O(9)-Fe(2)-O(6′)		91 (1)	2.80 (4)
O(9)-Fe(2)-O(10)		90 (1)	2.78 (4)
O(9)-Fe(2)-O(6′)		92 (1)	2.84 (4)
O(9)-Fe(2)-O(12)		85 (1)	2.68 (3)
O(8)-Fe(2)-O(7)		91 (1)	2.84 (5)
O(8)-Fe(2)-O(10)		88 (1)	2.79 (4)
O(8)-Fe(2)-O(6′)		90 (1)	2.84 (4)
O(8)-Fe(2)-O(12)		93 (1)	2.94 (4)
O(7)-Fe(2)-O(6′)		91 (1)	2.86 (4)
O(7)-Fe(2)-O(12)		89 (1)	2.83 (4)
O(10)-Fe(2)-O(6′)		90 (1)	2.86 (3)
O(10)-Fe(2)-O(12)		90 (1)	2.88 (4)
Fe(2′) Polyhedron			
Fe(2′)-O(12′)	1.90 (3)		
Fe(2′)-O(7′)	1.94 (3)		
Fe(2′)-O(8′)	1.99 (3)		
Fe(2′)-O(10′)	2.03 (4)		
Fe(2′)-O(9′)	2.05 (4)		
Fe(2′)-O(6)	2.05 (3)		
O(12′)-Fe(2′)-O(7′)		91 (1)	2.74 (4)
O(12′)-Fe(2′)-O(8′)		92 (1)	2.79 (4)
O(12′)-Fe(2′)-O(10′)		100 (2)	3.02 (5)
O(12′)-Fe(2′)-O(9′)		94 (1)	2.90 (4)
O(7′)-Fe(2′)-O(8′)		87 (1)	2.71 (4)
O(7′)-Fe(2′)-O(9′)		90 (1)	2.82 (4)
O(7′)-Fe(2′)-O(6)		89 (1)	2.80 (4)
O(8′)-Fe(2′)-O(10′)		91 (2)	2.87 (5)
O(8′)-Fe(2′)-O(6)		92 (1)	2.92 (4)
O(10′)-Fe(2′)-O(9′)		90 (1)	2.89 (6)
O(10′)-Fe(2′)-O(6)		80 (1)	2.62 (4)
O(9′)-Fe(2′)-O(6)		81 (1)	2.67 (4)
Fe(3) Polyhedron			
Fe(3)-O(4)	1.95 (3)		
Fe(3)-O(5)	1.96 (3)		
Fe(3)-O(1)	1.97 (3)		
Fe(3)-O(3)	2.01 (3)		
Fe(3)-O(2)	2.07 (3)		
Fe(3)-O(11′)	2.09 (3)		
O(4)-Fe(3)-O(5)		91 (1)	2.80 (4)
O(4)-Fe(3)-O(3)		98 (1)	3.00 (5)
O(4)-Fe(3)-O(2)		88 (1)	2.79 (4)
O(4)-Fe(3)-O(11′)		86 (1)	2.77 (4)
O(5)-Fe(3)-O(1)		90 (1)	2.78 (4)
O(5)-Fe(3)-O(3)		92 (1)	2.86 (4)
O(5)-Fe(3)-O(2)		93 (1)	2.93 (4)
O(1)-Fe(3)-O(3)		85 (1)	2.68 (4)
O(1)-Fe(3)-O(2)		89 (1)	2.84 (5)
O(1)-Fe(3)-O(11′)		92 (1)	2.92 (4)
O(3)-Fe(3)-O(11′)		91 (1)	2.92 (4)
O(2)-Fe(3)-O(11′)		85 (1)	2.80 (4)
Fe(3′) Polyhedron			
Fe(3′)-O(5′)	1.94 (3)		
Fe(3′)-O(11)	1.94 (3)		
Fe(3′)-O(2′)	1.94 (3)		
Fe(3′)-O(3′)	1.96 (3)		
Fe(3′)-O(1′)	1.97 (3)		
Fe(3′)-O(4′)	2.00 (3)		
O(5′)-Fe(3′)-O(2′)		87 (1)	2.66 (4)
O(5′)-Fe(3′)-O(3′)		96 (1)	2.90 (4)
O(5′)-Fe(3′)-O(1′)		90 (1)	2.76 (4)
O(5′)-Fe(3′)-O(4′)		95 (1)	2.90 (4)
O(11)-Fe(3′)-O(2′)		92 (1)	2.80 (4)
O(11)-Fe(3′)-O(3′)		86 (1)	2.65 (4)
O(11)-Fe(3′)-O(1′)		84 (1)	2.62 (4)
O(11)-Fe(3′)-O(4′)		91 (1)	2.82 (4)
O(2′)-Fe(3′)-O(1′)		91 (1)	2.79 (4)
O(2′)-Fe(3′)-O(4′)		92 (1)	2.83 (4)
O(3′)-Fe(3′)-O(1′)		93 (1)	2.86 (3)
O(3′)-Fe(3′)-O(4′)		85 (1)	2.64 (4)
Fe(4) Polyhedron			
Fe(4)-O(20)	1.91 (3)		
Fe(4)-O(24)	1.93 (2)		
Fe(4)-O(19)	1.99 (4)		
Fe(4)-O(22)	2.00 (2)		
Fe(4)-O(21)	2.03 (4)		
Fe(4)-O(18′)	2.08 (3)		
O(20)-Fe(4)-O(24)		91 (1)	2.74 (3)
O(20)-Fe(4)-O(19)		98 (1)	2.95 (5)
O(20)-Fe(4)-O(22)		84 (1)	2.61 (4)
O(20)-Fe(4)-O(18′)		95 (1)	2.94 (4)
O(24)-Fe(4)-O(19)		87 (1)	2.70 (4)
O(24)-Fe(4)-O(22)		95 (1)	2.90 (3)
O(24)-Fe(4)-O(21)		94 (1)	2.91 (4)
O(19)-Fe(4)-O(21)		91 (2)	2.87 (5)
O(19)-Fe(4)-O(18′)		85 (1)	2.74 (4)
O(22)-Fe(4)-O(21)		87 (1)	2.76 (5)
O(22)-Fe(4)-O(18′)		93 (1)	2.96 (3)
O(21)-Fe(4)-O(18′)		82 (1)	2.68 (5)
Fe(4′) Polyhedron			
Fe(4′)-O(18)	1.92 (3)		
Fe(4′)-O(21′)	1.93 (3)		
Fe(4′)-O(19′)	1.95 (3)		
Fe(4′)-O(24′)	2.03 (4)		
Fe(4′)-O(22′)	2.05 (3)		
Fe(4′)-O(20′)	2.09 (3)		
O(18)-Fe(4′)-O(21′)		95 (1)	2.85 (4)
O(18)-Fe(4′)-O(19′)		90 (1)	2.74 (4)
O(19′)-Fe(4′)-O(24′)		92 (1)	2.86 (5)

Table III (*Continued*)

	angle	edge		angle	edge
O(18)-Fe(4′)-O(22′)	87 (1)	2.74 (4)			
O(18)-Fe(4′)-O(20′)	83 (1)	2.67 (4)	O(19′)-Fe(4′)-O(20′)	92 (1)	2.91 (5)
O(21′)-Fe(4′)-O(19′)	91 (1)	2.76 (4)	O(24′)-Fe(4′)-O(22′)	91 (1)	2.91 (5)
O(21′)-Fe(4′)-O(24′)	89 (1)	2.79 (4)	O(24′)-Fe(4′)-O(20′)	92 (1)	2.96 (4)
O(21′)-Fe(4′)-O(22′)	85 (1)	2.70 (4)	O(22′)-Fe(4′)-O(20′)	92 (1)	2.98 (4)

[a] Numbers in parentheses are estimated standard deviations in the last significant figure.

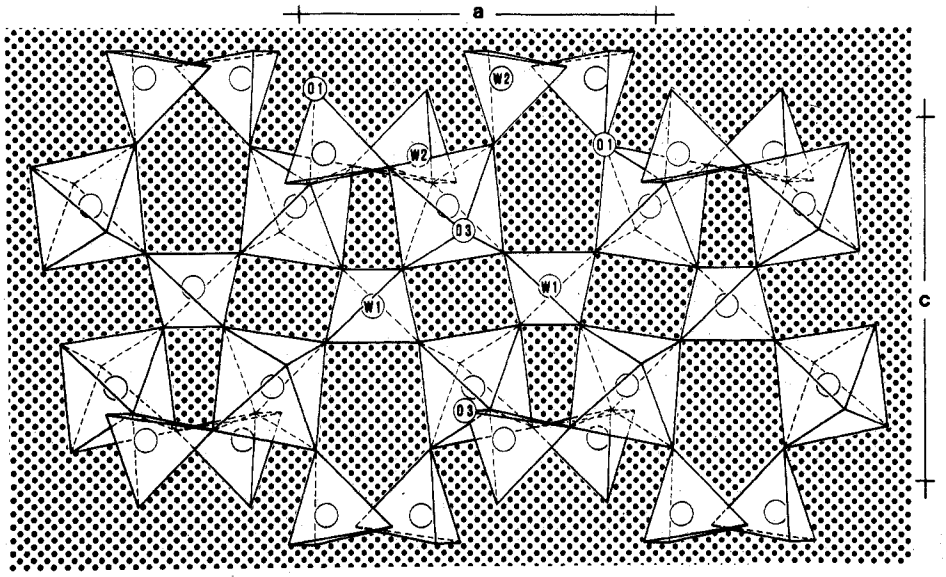

Figure 1. Fragment of a chainlike structure comprising layers in the a–c plane of $Sc_2(WO_4)_3$.

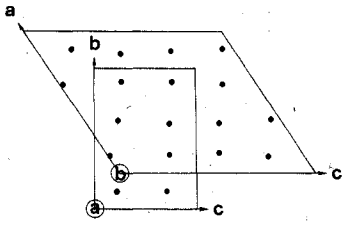

Figure 2. Projection of the pseudoorthorhombic unit cell of $Fe_2(MoO_4)_3$ upon the a–c plane of the monoclinic cell. The solid circles represent iron atoms.

and a brief examination of the oxygen temperature factors indicated O(14) as a likely candidate for relocation. The refinement was continued until convergence at $R = 0.049$ and $R_w = 0.068$.

At this stage, conversion was made from $P2_1/a$ to the true space group $P2_1$. Positional parameters were derived by an examination of a plot of the iron atoms projected onto the a–c plane. The coordinates x, y, and z of the space group $P2_1/a$ become $(x - 0.25, y, z)$ and $(x + 0.25, 0.5 - y, z)$ in the space group $P2_1$. The y coordinate of Fe(1) was held invariant in order to define the origin. Isotropic least-squares refinement with corrections for secondary extinction and anomalous dispersion converged to final $R = 0.041$ and $R_w = 0.055$ on the basis of a data to parameter ratio of 9:1 for 273 independently varied parameters. A refinement of the enantiomorph did not give a significantly lower R value. In this refinement, the maximum extinction correction[14] was 37% of $|F_c|$ for the $\bar{4}02$ reflection. The lower R value found in $P2_1$ vs. $P2_1/a$ was determined to be significant at the 0.995 confidence level.[15] Table I presents the final atomic coordinates and isotropic thermal parameters.

At the completion of the refinement, four oxygens were found to have negative isotropic temperature factors [O(9), O(10), O(13), O(15)], undoubtedly due to the large correlation coefficients between pairs of oxygens which arise as a direct result of the reduction in space group symmetry. (All such pairs of atoms are indicated by primed numbers.)

In order to obtain the complete correlation matrix necessary to compute standard deviations for interatomic distances and angles, the least-squares program was expanded to permit refinement of all atomic and thermal parameters simultaneously. After a single cycle of refinement using this modified program, standard deviations were computed with the function and error program ORFFE.[16]

Results and Discussion

Each of the eight cyrstallographically unique iron atoms is essentially octahedrally coordinated by six oxygen atoms at an overall average distance of 1.992 Å. The twelve molybdenum atoms are in rather distorted oxygen tetrahedra with an overall average Mo–O distance of 1.756 Å. Table II lists the bond distances and angles for the molybdenum tetrahedra, and Table III presents those for the iron polyhedra.

Each oxygen atom links an FeO_6 octahedron with one MoO_4 tetrahedron. This leads to a rather open structure (vide infra) in which the nearest Fe–Fe distance is 5.03 Å. Table IV presents the angles and distances about each of the oxygen atoms.

All of the type C compounds of this stoichiometry[1] appear to be of the same structure type. Two compounds particularly relevant to this study are $Sc_2(WO_4)_3$ and orthorhombic Fe_2-

(14) W. H. Zachariasen, *Acta Crystallogr.*, **23**, 558 (1967); *Acta Crystallogr., Sect. A*, **A24**, 324 (1968).
(15) W. Hamilton, *Acta Crystallogr.*, **18**, 502 (1965).
(16) W. R. Busing, K. O. Martin, and H. A. Levy, "ORFFE", Report ORNL-TM-306, Oak Ridge National Laboratory, Oak Ridge, TN, 1962.

Table IV. Bond Distances (Å), Bond Angles (Deg), and Polyhedral Edge Lengths (Å) for Anion Polyhedra[a]

	dist	angle	edge		dist	angle	edge
O(1)-Mo(4′)	1.82 (3)			O(12′)-Mo(2′)	1.79 (3)		
O(1)-Fe(3)	1.97 (3)			O(12′)-Fe(2′)	1.90 (3)		
Mo(4′)-O(1)-Fe(3)		153 (2)	3.68 (1)	Mo(2′)-O(12′)-Fe(2′)		144 (2)	3.51 (1)
O(1′)-Mo(4)	1.72 (3)			O(13)-Mo(1)	1.80 (3)		
O(1′)-Fe(3′)	1.97 (3)			O(13)-Fe(1)	1.99 (3)		
Mo(4)-O(1′)-Fe(3′)		162 (2)	3.65 (1)	Mo(1)-O(13)-Fe(1)		139 (1)	3.55 (1)
O(2)-Mo(4)	1.69 (3)			O(13′)-Mo(1′)	1.73 (4)		
O(2)-Fe(3)	2.07 (3)			O(13′)-Fe(1′)	2.03 (4)		
Mo(4)-O(2)-Fe(3)		138 (2)	3.51 (1)	Mo(1′)-O(13′)-Fe(1′)		136 (2)	3.50 (1)
O(2′)-Mo(4′)	1.83 (3)			O(14)-Mo(1′)	1.76 (3)		
O(2′)-Fe(3′)	1.94 (3)			O(14)-Fe(1)	2.03 (4)		
Mo(4′)-O(2′)-Fe(3′)		138 (1)	3.51 (1)	Mo(1′)-O(14)-Fe(1)		154 (1)	3.69 (1)
O(3)-Mo(3)	1.75 (3)			O(14′)-Mo(1)	1.74 (4)		
O(3)-Fe(3)	2.01 (3)			O(14′)-Fe(1′)	1.96 (4)		
Mo(3)-O(3)-Fe(3)		137 (1)	3.50 (1)	Mo(1)-O(14′)-Fe(1′)		156 (2)	3.62 (1)
O(3′)-Mo(3′)	1.81 (3)			O(15)-Mo(6)	1.82 (4)		
O(3′)-Fe(3′)	1.96 (3)			O(15)-Fe(1)	1.92 (4)		
Mo(3′)-O(3′)-Fe(3′)		136 (1)	3.49 (1)	Mo(6)-O(15)-Fe(1)		140 (2)	3.52 (1)
O(4)-Mo(5)	1.72 (2)			O(15′)-Mo(6′)	1.71 (3)		
O(4)-Fe(3)	1.95 (3)			O(15′)-Fe(1′)	2.03 (3)		
Mo(5)-O(4)-Fe(3)		157 (2)	3.60 (1)	Mo(6′)-O(15′)-Fe(1′)		144 (1)	3.56 (1)
O(4′)-Mo(5′)	1.78 (3)			O(16)-Mo(2)	1.78 (4)		
O(4′)-Fe(3′)	2.00 (3)			O(16)-Fe(1)	2.00 (4)		
Mo(5′)-O(4′)-Fe(3′)		151 (2)	3.65 (1)	Mo(2)-O(16)-Fe(1)		131 (2)	3.45 (1)
O(5)-Mo(6)	1.72 (3)			O(16′)-Mo(2′)	1.77 (3)		
O(5)-Fe(3)	1.96 (3)			O(16′)-Fe(1′)	1.98 (3)		
Mo(6)-O(5)-Fe(3)		169 (2)	3.67 (1)	Mo(2′)-O(16′)-Fe(1′)		139 (2)	3.51 (1)
O(5′)-Mo(6′)	1.78 (3)			O(17)-Mo(3)	1.73 (2)		
O(5′)-Fe(3′)	1.94 (3)			O(17)-Fe(1)	1.98 (2)		
Mo(6′)-O(5′)-Fe(3′)		164 (2)	3.68 (1)	Mo(3)-O(17)-Fe(1)		141 (1)	3.49 (1)
O(6)-Mo(3)	1.81 (2)			O(17′)-Mo(3′)	1.81 (3)		
O(6)-Fe(2′)	2.05 (3)			O(17′)-Fe(1′)	1.97 (3)		
Mo(3)-O(6)-Fe(2′)		155 (1)	3.76 (1)	Mo(3′)-O(17′)-Fe(1′)		136 (1)	3.51 (1)
O(6′)-Mo(3′)	1.72 (3)			O(18)-Mo(6)	1.79 (3)		
O(6′)-Fe(2)	2.02 (3)			O(18)-Fe(4′)	1.92 (3)		
Mo(3′)-O(6′)-Fe(2)		169 (2)	3.72 (1)	Mo(6)-O(18)-Fe(4′)		174 (2)	3.70 (1)
O(7)-Mo(6)	1.78 (3)			O(18′)-Mo(6′)	1.70 (2)		
O(7)-Fe(2)	1.99 (3)			O(18′)-Fe(4)	2.08 (3)		
Mo(6)-O(7)-Fe(2)		145 (2)	3.60 (1)	Mo(6′)-O(18′)-Fe(4)		158 (2)	3.71 (1)
O(7′)-Mo(6′)	1.79 (3)			O(19)-Mo(3)	1.77 (4)		
O(7′)-Fe(2′)	1.94 (3)			O(19)-Fe(4)	1.99 (4)		
Mo(6′)-O(7′)-Fe(2′)		148 (2)	3.59 (1)	Mo(3)-O(19)-Fe(4)		146 (2)	3.60 (1)
O(8)-Mo(2)	1.75 (4)			O(19′)-Mo(3′)	1.76 (3)		
O(8)-Fe(2)	1.99 (4)			O(19′)-Fe(4′)	1.95 (3)		
Mo(2)-O(8)-Fe(2)		143 (2)	3.54 (1)	Mo(3′)-O(19′)-Fe(4′)		146 (2)	3.55 (1)
O(8′)-Mo(2′)	1.78 (3)			O(20)-Mo(5)	1.72 (3)		
O(8′)-Fe(2′)	1.99 (3)			O(20)-Fe(4)	1.91 (3)		
Mo(2′)-O(8′)-Fe(2′)		139 (2)	3.53 (1)	Mo(5)-O(20)-Fe(4)		151 (2)	3.52 (1)
O(9)-Mo(4′)	1.83 (2)			O(20′)-Mo(5′)	1.78 (3)		
O(9)-Fe(2)	1.93 (2)			O(20′)-Fe(4′)	2.09 (3)		
Mo(4′)-O(9)-Fe(2)		148 (1)	3.61 (1)	Mo(5′)-O(20′)-Fe(4′)		139 (2)	3.64 (1)
O(9′)-Mo(4)	1.68 (4)			O(21)-Mo(1)	1.70 (4)		
O(9′)-Fe(2′)	2.05 (4)			O(21)-Fe(4)	2.03 (4)		
Mo(4)-O(9′)-Fe(2′)		153 (2)	3.63 (1)	Mo(1)-O(21)-Fe(4)		166 (2)	3.69 (1)
O(10)-Mo(4)	1.82 (3)			O(21′)-Mo(1′)	1.74 (2)		
O(10)-Fe(2)	2.02 (3)			O(21′)-Fe(4′)	1.93 (3)		
Mo(4)-O(10)-Fe(2)		132 (2)	3.50 (1)	Mo(1′)-O(21′)-Fe(4′)		159 (2)	3.61 (1)
O(10′)-Mo(4′)	1.66 (4)			O(22)-Mo(1′)	1.79 (2)		
O(10′)-Fe(2′)	2.03 (4)			O(22)-Fe(4)	2.00 (2)		
Mo(4′)-O(10′)-Fe(2′)		137 (2)	3.44 (1)	Mo(1′)-O(22)-Fe(4)		144 (1)	3.60 (1)
O(11)-Mo(2)	1.85 (3)			O(22′)-Mo(1)	1.70 (4)		
O(11)-Fe(3′)	1.94 (3)			O(22′)-Fe(4′)	2.05 (3)		
Mo(2)-O(11)-Fe(3′)		167 (2)	3.76 (1)	Mo(1)-O(22′)-Fe(4′)		155 (2)	3.66 (1)
O(11′)-Mo(2′)	1.66 (3)			O(23)-Mo(5)	1.76 (3)		
O(11′)-Fe(3)	2.09 (3)			O(23)-Fe(1′)	2.02 (3)		
Mo(2′)-O(11′)-Fe(3)		167 (2)	3.72 (1)	Mo(5)-O(23)-Fe(1′)		168 (2)	3.75 (1)
O(12)-Mo(2)	1.72 (3)			O(23′)-Mo(5′)	1.74 (3)		
O(12)-Fe(2)	2.05 (3)			O(23′)-Fe(1)	2.05 (3)		
Mo(2)-O(12)-Fe(2)		147 (2)	3.62 (1)	Mo(5′)-O(23′)-Fe(1)		162 (2)	3.74 (1)

Table IV (*Continued*)

	dist	angle	edge		dist	angle	edge
O(24)-Mo(5)	1.82 (2)			O(24')-Mo(5')	1.63 (4)		
O(24)-Fe(4)	1.93 (2)			O(24')-Fe(4')	2.03 (4)		
Mo(5)-O(24)-Fe(4)		154 (1)	3.66 (1)	Mo(5')-O(24')-Fe(4')		161 (2)	3.61 (1)

[a] Numbers in parentheses are estimated standard deviations in the last significant figure.

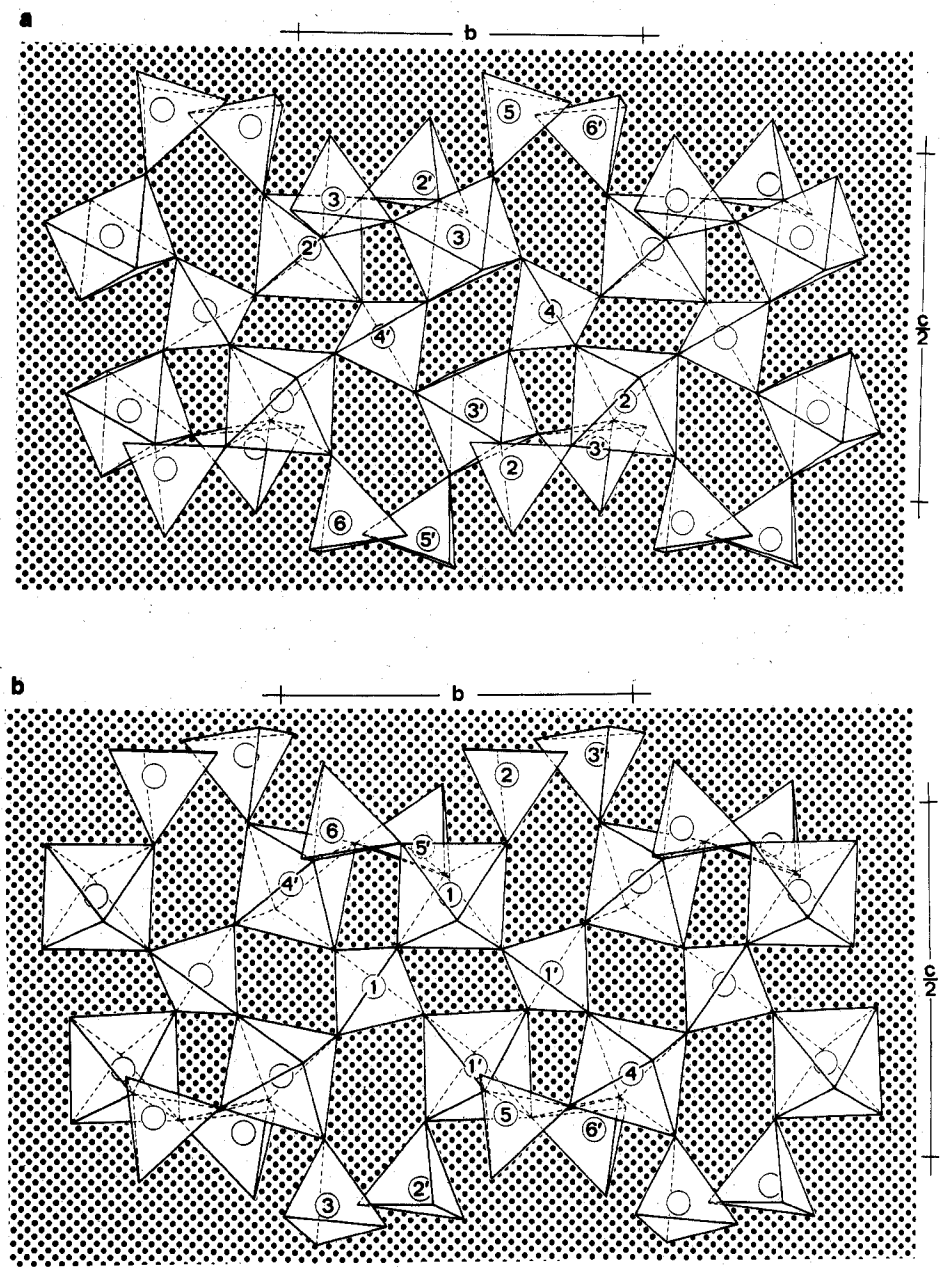

Figure 3. Equivalent segments of the symmetry-inequivalent A and B chains (a and b, respectively) which comprise the structure of monoclinic $Fe_2(MoO_4)_3$.

$(MoO_4)_3$, because of the close agreement in lattice parameters with those of the observed pseudoorthorhombic subcell:

	a, Å	*b*, Å	*c*, Å
pseudoorthorhombic setting	9.20	12.78	9.08
$Sc_2(WO_4)_3$	9.60	13.33	9.51
orthorhombic $Fe_2(MoO_4)_3$	9.2	12.8	9.2

Since there seems to be a nondestructive phase transition from orthorhombic $Fe_2(MoO_4)_3$ to the monoclinic form at 518 °C,[5] this transition should occur by distorting the atomic arrangement of the orthorhombic form into the lower monoclinic symmetry. With the assumption of such a structural similarity, a model of $Sc_2(WO_4)_3$ was constructed and examined in conjunction with precession photographs of $Sc_2(WO_3)_4$ and monoclinic $Fe_2(MoO_4)_3$ to yield a self-consistent model for the molybdate. Therefore, we will begin the description of the structure of monoclinic $Fe_2(MoO_4)$ by first describing the $Sc_2(WO_4)_3$ structure. In this fashion the effects of the symmetry-lowering distortions can be examined.

The scandium tungstate structure has been shown[2] to consist

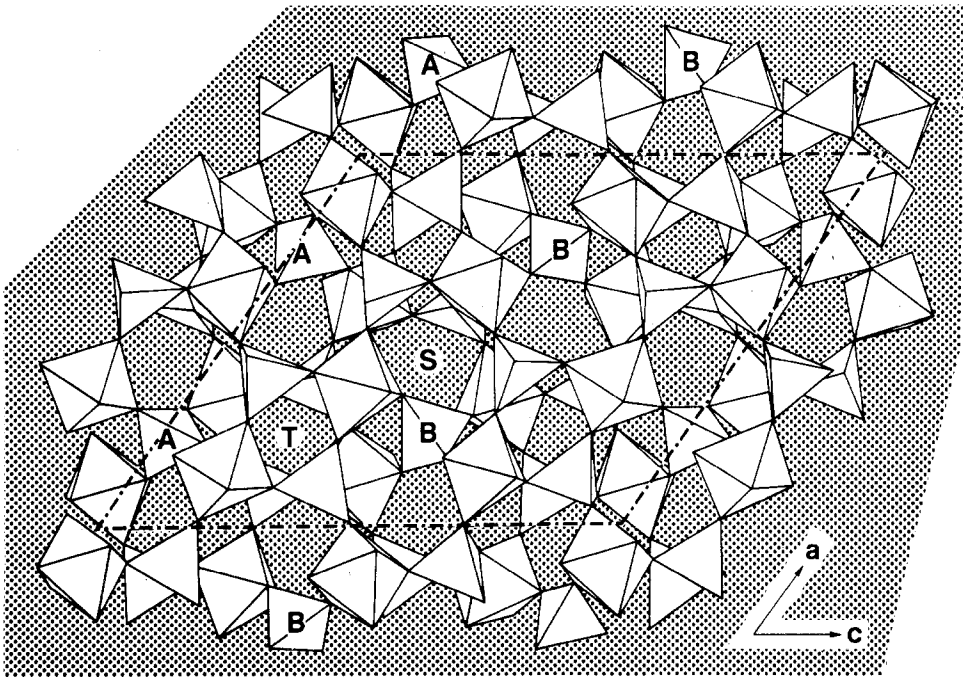

Figure 4. End-on view of the A and B chains (down the *b* axis) illustrating, in part, the interchain and interlayer linkages and the two channellike cavities, S and T (see text), formed due to the low packing density of polyhedra.

of ScO_6 octahedra and WO_4 tetrahedra linked together via their vertices in such a fashion that they may be considered to form layers in the orthorhombic *a*–*c* plane. A fragment of one such layer is shown in Figure 1. Adjacent layers in the *b* direction are related to each other by a translation of $c/2$. Such a translation permits the one, as yet unshared, outwardly pointing vertex of every scandium octahedron [O(3)] to join with the one unshared vertex of a W(2) tetrahedron in the adjacent layer. This is the only link between adjacent layers.

For comparison of this structure to that of $Fe_2(MoO_4)_3$, a division of the layers into more basic units is necessary. These units can be arrived at simply by severing all links involving O(1) within each layer in $Sc_2(WO_4)_3$. Such a division yields the basic unit, a chain based on a W(1) "backbone" containing all ScO_6 octahedra which extends parallel to the *a* axis (see Figure 1).

To this point, if symmetry differences and absolute conformations are neglected, the structures are identical and need only to be related by unit cells. The relationships between the monoclinic and orthorhombic cell axes are

$$a_M = b_O - c_O \qquad b_M = a_O \qquad c_M = 2c_O$$

where the subscripts M and O refer to the orthorhombic and monoclinic cells, respectively. Figure 2 shows the projection of the pseudoorthorhombic unit cell upon the *a*–*c* plane of the monoclinic cell with the iron atoms represented by solid circles. From this point on, all references will be made to the monoclinic axes.

The conversion to these axes is, of course, necessitated by the loss of symmetry when the structure distorts from orthorhombic to monoclinic. In addition to this, the loss of symmetry causes equivalent chains in the orthorhombic cell to form two inequivalent chains in the monoclinic cell. For ease of reference, these two symmetrically distinct chains will be referred to as chain A and chain B. Equivalent segments of both chains are shown respectively, in parts a and b of Figure 3. A direct comparison of these two chains with each other and with the orthorhombic chain appearing in Figure 1 reveals obvious similarities. Chain B compares very closely to the orthorhombic chain with only a minimal amount of apparent distortion as can be seen by inspecting the bond lengths and angles (Table II). Chain A, in contrast, is grossly distorted, as indicated by the bond lengths and angles within this chain.

In forming a layer, these two chains stack in an alternating ...ABAB... fashion in the *b*–*c* plane. Since the *c* axis of the monoclinic cell is parallel to the *c* axis of the orthorhombic cell and is double this axis, the translation of adjacent layers becomes $^1/_4c$ in the monoclinic cell.

The resulting sequencing of chains and layers produces an interesting feature within the structure—layers in the *a*–*b* plane comprised alternately of only A or B chains. This is shown in Figure 4, an end-on view of the A and B chains (looking down *b*), illustrating, in part, the interchain and interlayer linkages. Another characteristic of this and related structures is the low packing density of polyhedra resulting in a rather open structure. Two channellike cavities extend through the structure parallel to the *b* axis. The channels labeled S are formed between alternating layers while those labeled T occur between chains within a layer.

It was pointed out by Wells[17] that the removal of the M′ (eight-coordinated) atoms in the garnet structure type $M'_3M''_2(M'''O_4)_3$ results in a three-dimensional framework built of $M''O_6$ octahedra joined to six others through vertex-sharing $M'''O_4$ tetrahedra. Such a framework is known to exist independently of the garnet structure in a much distorted form in $Al_2(WO_4)_3$.[18]

Noting the similarity of this framework to the structure of $Fe_2(MoO_3)_4$, a detailed structural comparison was conducted by Plyasova et al.[19] A presentation of this analysis in light of the present study is illustrated in Figure 5, which shows the relationship of the pseudocubic garnet-type unit cell to the unit cell of the monoclinic molybdate. The solid circles represent iron atoms and the open circles the ideal iron positions in the garnet framework. The solid squares on each layer show the

(17) A. F. Wells, "Structural Inorganic Chemistry", 4th ed., Oxford University Press, Oxford, 1975, p 500.
(18) J. J. De Boer, *Acta Crystallogr., Sect. B*, **B30**, 1878 (1974).
(19) L. M. Plyasova, S. V. Borisov, and N. V. Belov, *Sov. Phys.—Crystallogr. (Engl. Transl.)*, **12**, 25 (1967).

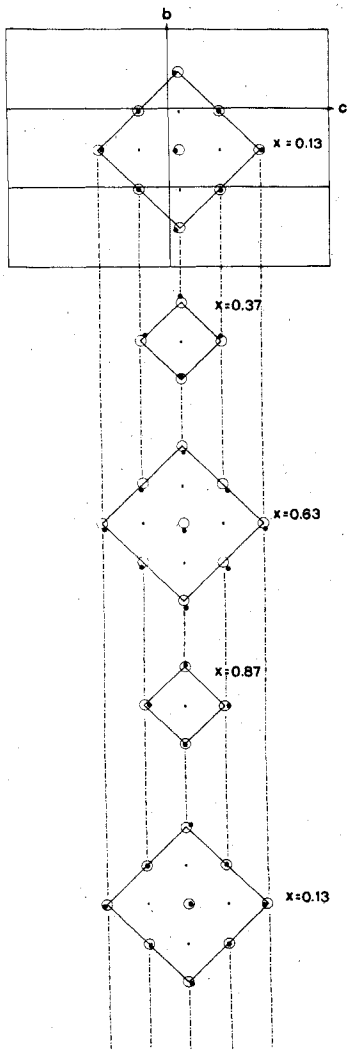

Figure 5. Relationship of the pseudocubic garnet-type unit cell to the unit cell of the monoclinic molybdate. Open circles and solid squares represent the ideal positions within the garnet framework of iron atoms in each layer and in the adjacent layers, respectively. Solid circles represent actual iron atom positions (x values shown are the average values for iron atoms within each layer with respect to the monoclinic cell).

ideal positions of the iron atoms in the adjacent layers. The x value given for each layer represents the average value of the actual iron atoms within a layer of the monoclinic cell. The maximal deviation from the average value is ±0.013 (or 0.17 Å). Further comparison of these two structures does not indicate a simple direct correlation between the tetrahedral groups and the polyhedral linkages.

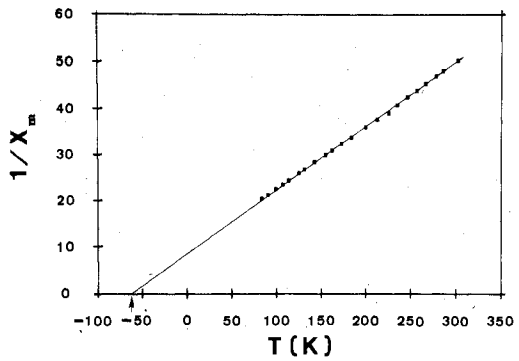

Figure 6. Plot of $1/\chi_m$ vs. T for $Fe_2(MoO_4)_3$.

Figure 6 presents the results of the magnetic susceptibility measurements as a plot of $1/\chi_m$ vs. T. This plot is typical of an antiferromagnetic material with a temperature intercept (Θ) of −62.7 K and a paramagnetic moment of 5.57 μ_B/Fe atom, a value typical of Fe^{3+} in oxidic materials.

Acknowledgment. We thank The Standard Oil Co. of Ohio for partial financial support and, in particular, Dr. Robert K. Grasselli for fruitful discussions. Magnetic susceptibility measurements were made at Brown University through the courtesy of Professor Aaron Wold. Computations were carried out in the Computer Center of the University of Connecticut.

Appendix

During the final preparation of this paper, Chen[20] reported an investigation in which crystallographic data were collected on a crystal of $Fe_2(MoO_4)_3$ which exhibited "pseudo" $P2_1$ systematic absences. It was reported that $h0l$ reflections with *both* h and l odd were systematically absent, which is a pseudoextinction condition. As a result, Chen[20] proposed a mechanism for twinning on the monoclinic ac plane in $P2_1/a$ to account for our assignment of the lower symmetry space group.

However, a careful examination of our data in light of this claim reveals that, of the 34 observed reflections of the type $h0l$ (h odd), fully 30 had *both* h and l odd, in sharp contrast to their results. Therefore, Chen's twinning mechanism does not account for our data.

In light of this discrepancy we calculated structure factors by using Chen's twinning mechanism and found that the only structure factors systematically absent were the class $h00$ (h odd). Although we cannot conclusively prove that our crystal is untwinned, we can rule out Chen's mechanism.

Registry No. $Fe_2(MoO_4)_3$, 13769-81-8.

Supplementary Material Available: A listing of calculated and observed structure factors (12 pages). Ordering information is given on any current masterhead page.

(20) H.-Y. Chen, *Mater. Res. Bull.*, **14**, 1583 (1979).